RESEARCH ARTICLE

JOURNAL OF **morphology** WILEY

Comparative anatomy and functional implications of variation in the buccal mass in coleoid cephalopods

Marjorie Roscian[1,2] | Louise Souquet[3] | Anthony Herrel[2,4] |
Theodore Uyeno[5] | Dominique Adriaens[4] | Barbara De Kegel[4] | Isabelle Rouget[1]

[1]Centre de Recherche en Paléontologie-Paris (CR2P), Muséum National d'Histoire Naturelle, CNRS, Sorbonne Université, Paris, France

[2]Mécanismes Adaptatifs et Evolution (Mecadev), Muséum National d'Histoire Naturelle, CNRS, Bâtiment d'Anatomie Comparée, Paris, France

[3]Department of Mechanical Engineering, University College London, London, UK

[4]Evolutionary Morphology of Vertebrates, Ghent University, Ghent, Belgium

[5]Department of Biology, Valdosta State University, Valdosta, USA

Correspondence
Marjorie Roscian, Centre de Recherche en Paléontologie-Paris (CR2P), Muséum National d'Histoire Naturelle, CNRS, Sorbonne Université, 8 rue Buffon, CP 38, 75005 Paris, France.
Email: marjorie.roscian@gmail.com

Abstract

In contrast to the well-studied articulated vertebrate jaws, the structure and function of cephalopod jaws remains poorly known. Cephalopod jaws are unique as the two jaw elements do not contact one another, are embedded in a muscular mass and connected through a muscle joint. Previous studies have described the anatomy of the buccal mass muscles in cephalopods and have proposed variation in muscle volume depending on beak shape. However, the general structure of the muscles has been suggested to be similar in octopuses, squids, and cuttlefish. Here we provide a quantitative analysis of the variation in the buccal mass of coleoids using traditional dissections, histological sections and contrast-enhanced computed tomography scans. Our results show that the buccal mass is composed of four main homologous muscles present in both decapodiforms and octopodiforms as suggested previously. However, we also report the presence of a muscle uniquely present in octopodiforms (the postero-lateral mandibular muscle). Our three dimensional reconstructions and quantitative analyses of the buccal mass muscles pave the way for future functional analyses allowing to better model jaw closing in coleoids. Finally, our results suggest differences in beak and muscle function that need to be validated using future in vivo functional analyses.

KEYWORDS
cephalopod beak, CT scan, decapodiforms, dissection, muscle, octopodiforms

1 | INTRODUCTION

While the articulated jaw is an effective structure to hold, kill and cut prey, there is a wide variety of ways to perform these functions. Whereas, toothed jaws are most commonly observed in vertebrates, variations exist such as beaks in birds and turtles, toothless jaws in some amphibians, or horny teeth without jaws in lampreys (Clark & Uyeno, 2019; Davit-Béal et al., 2009; Louchart & Viriot, 2011). Among invertebrates, the strategies are similarly diversified. In molluscs, the key structure is the radula, a ribbon armed with multiple small chitinous teeth that can be rasped against the substrate or the prey (Messenger & Young, 1999; Scheel et al., 2020). Except in cephalopods, the radula is rarely associated with a pair of jaws. Indeed, the cephalopod feeding apparatus is a

---

unique biological structure in living organisms (Figure 1), composed of not only a radula, but also a pair of jaws, called beaks, embedded in a large muscular mass (Clarke, 1986; Tanabe & Fukuda, 1999, 2010; Williams, 1909). Surprisingly, the two beaks are not in contact with one another except for the biting surfaces, and articulate by means of a muscular joint, known as a muscle articulation, that allows a great freedom of motion (Kear, 1994; Uyeno & Kier, 2005, 2007). The beaks and their muscles surround the radular apparatus, with the upper beak nested inside the lower one when the beaks are closed (Nixon, 2015). Within the buccal cavity formed by the beaks lies a singular submandibular salivary gland. Two pairs of salivary glands are found outside the buccal cavity: The anterior pair is located on the posterior surface of the buccal mass, and the posterior pair is located in the mantle. The posterior pair, which is present in most cephalopods, produces a venom that can kill, immobilize, and/or predigest the prey, facilitating food intake (Altman & Nixon, 1970; Cooke et al., 2009; Nixon, 1979, 1980).

Whereas the structure of the buccal mass has been described in some detail, the joint and the mechanism underlying jaw motion remain poorly understood. Previous functional morphological studies have proposed a bite cycle in which the upper jaw would be the main actor of the bite, widening the gap, retracting and closing onto the lower jaw (Boyle et al., 1979; Kear, 1994; Uyeno & Kier, 2007). Electromyographic recordings of the buccal muscles in vitro have partially validated these results. Nevertheless, the timing and degree

of activation of each of the muscles has not been described in detail, partly because our incomplete understanding of the buccal mass muscle anatomy. Kear (1994) performed a series of dissections and stated that all coleoids, the group containing the octopuses, squid, and cuttlefish, have an identical musculature. However, she described that the volume of the different muscles appeared to be dependent on the shape of the beaks. Like Boyle et al. (1979), Kear (1994) described three mandibular muscles: the Superior Mandibular Muscle (SMM) divided into three sections inserting onto the crest and walls of the upper beak; the Lateral Mandibular Muscle (LMM), a paired muscle on each side of the upper and lower beaks, and the inferior mandibular muscle (IMM), a paired muscle attaching to the lateral walls of the lower beak. This muscle was later renamed the Anterior Mandibular Muscle (AMM; Uyeno & Kier, 2005).

Kear (1994) suggested that the SMM is responsible for beak closure in combination with the LMM and IMM. However, she considered the latter two muscles to be less important. The LMM was identified by Kear (1994) and Uyeno and Kier (2007) as an opening muscle. A posterior part was suggested to cause beak opening when stimulated and was later identified as the Posterior Mandibular Muscle (PMM) by Uyeno and Kier (2005). Kear (1994) was the first to show that the beaks move differently depending on the area that was stimulated and that there is not a single pivot point but more generally an area in which the pivot point can be localized, subsequently described by Uyeno and Kier (2005) as a new type of
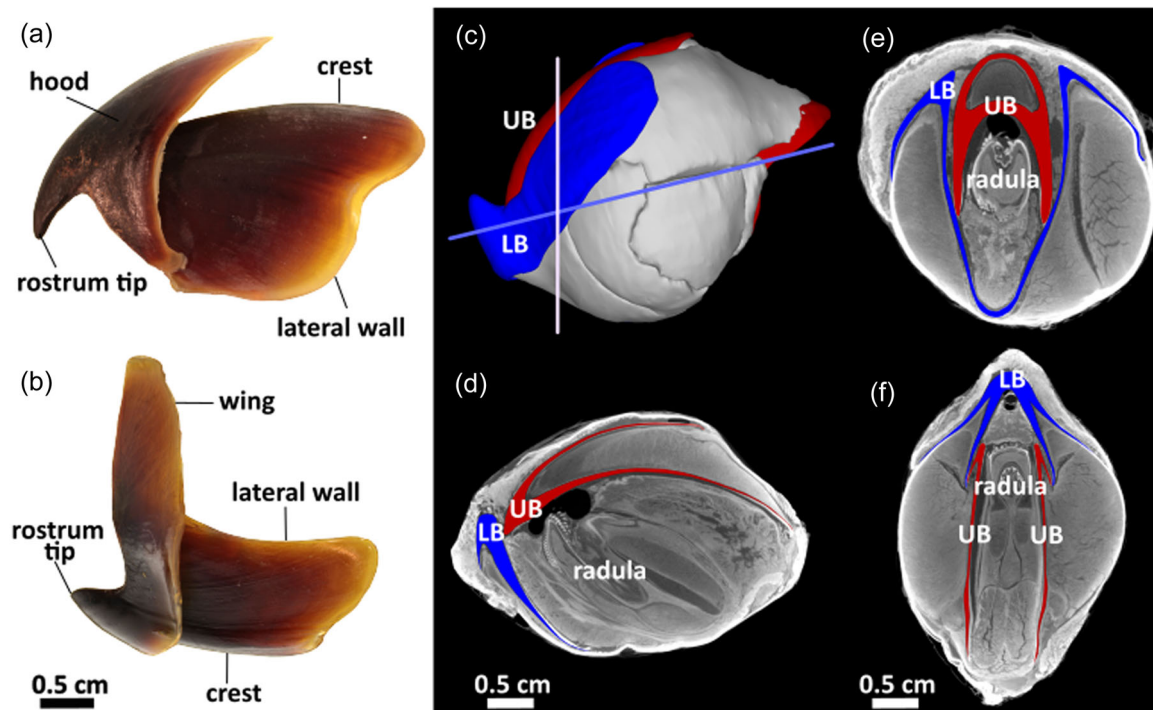
FIGURE 1 Anatomy of cephalopods beaks illustrated by *Sepia officinalis*. (a, b) Picture of the (a) upper beak and (b) lower beak in lateral view with the main morphological features. (c–f) Virtual section of the buccal mass, PMA-stained. (c) Volume rendering of the buccal mass with upper beak (UB) in red and lower beak (LB) in blue, the lines representing the illustrated frontal section (E, white line) and transversal section (F, blue line). (d) Sagittal section highlighting the position of the beaks. (e) Frontal section highlighting the position of the beaks. (f) Transversal section highlighting the position of the beaks.
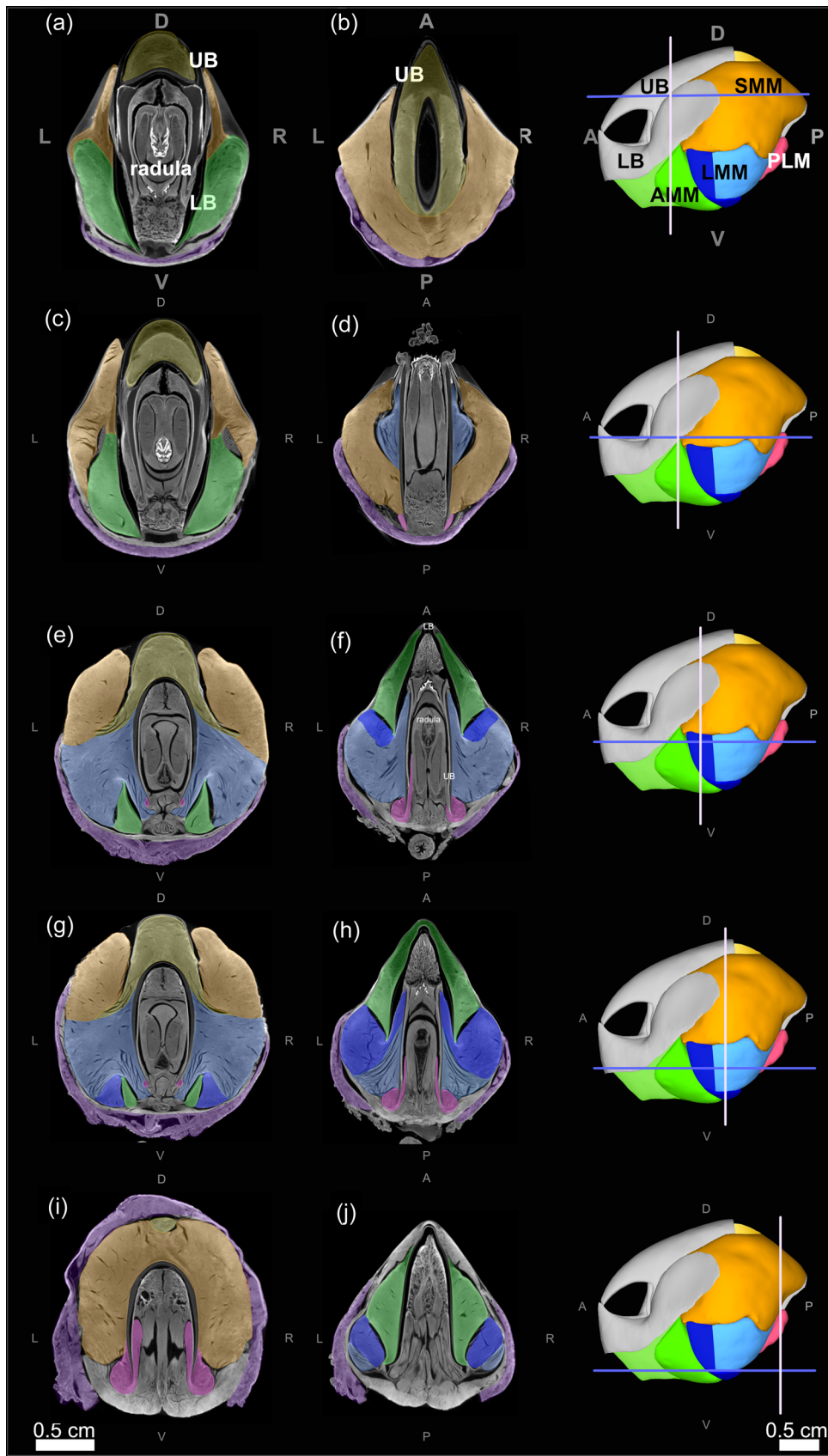
FIGURE 2 (See caption on next page)

joint formed by a muscular hydrostat, known as a muscle articulation (Uyeno & Clark, 2015; Uyeno & Kier, 2005, 2007, 2010). Based on the bite cycle proposed by Boyle et al. (1979), Kear (1994) and Uyeno and Kier (2007) identified the SMM as responsible for the closure of the beak. Yet, they also suggested a series of other movements such as scissor-like shearing, made possible by the five degrees of freedom of the upper beak and the multidirectional muscle fiber orientations (Uyeno & Kier, 2007). In contrast to the buccal mass, the radular apparatus of cephalopods has been described in the literature (Altman & Nixon, 1970; Nixon, 1979, 1985; Young, 1991) and its general function has been investigated (Voight et al., 2012).

Despite our apparent understanding of the main mandibular muscles and their function, the great variability of jaw shapes (Clarke, 1986; Roscian et al., 2022) raises the question of whether and how they are functionally related to variation in muscle size, architecture, and function (Kear, 1994). The aim of the present study was to describe the muscles of the buccal mass in coleoid cephalopods using three dimensional (3D) visualization techniques (contrast-enhanced computed tomography [CT] scans) coupled to dissections and serial histological sections.

2 | MATERIAL AND METHODS

At least one species of each main coleoid group was chosen for this study. When available, multiple species were dissected and scanned to investigate the variation between closely related species. For octopodiforms, specimens of the common octopus *Octopus vulgaris* Cuvier, 1797 were dissected (N = 1) and CT-scanned (N = 1). An individual of *Eledone cirrhosa* (Lamarck, 1798) was used for histological sectioning. For decapodiforms, *Sepia officinalis* Linnaeus, 1758 was used as representative of cuttlefish, CT-scanned (N = 1) and dissected (N = 3). *Illex coindetii* (Vérany, 1837) and *Dosidicus gigas gigas* (d'Orbigny, 1835), two species of squid belonging to the family Ommastrephidae, were used to represent squids for both dissections (N = 3 and 1, respectively) and contrast-enhanced CT-scanning (N = 1 for each species). All specimens were obtained commercially from local fishmongers and caught in French waters, except for the *Dosidicus gigas* specimen that was caught in the Gulf of California. The buccal masses were excised from the animal and fixed in 10% formaldehyde before being stored in 70% ethanol. Half of the specimens were dissected. Muscles were identified and the origin, insertion, and fiber orientation were recorded.

After dissection, individual muscles were weighed and placed in a 30% nitric acid solution for 72 h to separate the fibers by digestion of surrounding connective tissue allowing to measure their length. Fibers were then placed in a 50% glycerol solution and their length was measured using a camera lucida. Ten to fifteen individual fibers were measured and averaged for each muscle. Based on these measurements, the Physiological Cross Sectional Area (PCSA) of each muscle bundle was calculated (Haxton, 1944), using the equation:

$$PCSA = \frac{m}{\rho \cdot L}$$

where m is the muscle mass (g), ρ is the theoretical muscle density, and L is the fiber length. A muscle density (ρ) of 1.06 g/cm^3 was used as documented in (Denton and Gilpin Brown, 1973).

In parallel, a second set of fixed buccal masses were placed in an ethanol-based solution of phosphomolybdic acid (PMA) (5%, except for *Dosidicus gigas* which was stained using a 10% solution) allowing accurate soft tissue visualization using CT-scanning (Descamps et al. 2014). The speed by which the contrast agent penetrates the buccal mass depended on its size, freshness and fixation. The buccal masses were stained for 4–12 weeks. Buccal masses were scanned at the AST-RX platform of the Paris Natural History Museum using a GE phoenix v|tome|x L 240-180 micro-CT, except for *S. officinalis* which was scanned with a Nikon XT H 225 ST scanner (Nikon Metrology Ltd.) at University College London, department of Mechanical Engineering. CT parameters for each scan are given in Supporting Information online Material, Supporting Information: Table 1. Segmentation was done using the Materialize Mimics Software(v.21.0.0).

For histology, an additional fixed buccal mass of an *Eledone cirrhosa* was embedded in Technovit 7100 (methacrylate, Heraus-Kulzer) after dehydration and serially sectioned at 5 µm at Ghent University. One set of sections was stained with Toluidine Blue and another with Hematoxylin and Eosin stain.

3 | RESULTS

3.1 | *The buccal mass of decapodiforms: I. coindetii, Dosidicus gigas, and S. officinalis*

The buccal mass of decapodiforms is composed of four mandibular muscles, as described by Kear (1994) and expanded upon by Uyeno and Kier (2005). *I. coindetii* (Figure 2), *Dosidicus gigas* (Figure 3; Supporting Information online Material, Supporting Information: Figures S1, 2), and *S. officinalis* (Figure 4) present the same muscular organization which

FIGURE 2 Volume renderings and virtual sections illustrated in different orientations of *Illex coindetii* from microCT scan with PMA staining. On the right, the 3D model illustrates the section planes with frontal section (a–i, white lines) and transversal section (b–j, blue lines). The muscles are identified by colors. Superior Mandibular Muscle (SMM), lateral division, orange; SMM, inner division, yellow; Anterior Mandibular Muscle (AMM), green; Lateral Mandibular Muscle (LMM), main part, light blue; LMM, anterior section, deep blue; Postero-Lateral Muscle (PLM), pink; Posterior Mandibular Muscle (PMM), purple. The PMM is not illustrated on the 3D model as it surrounds the entire muscle mass and would have masked the other structures. It is visible on the sections. 3D, three dimensional; LB, Lower beak; UB, Upper beak.
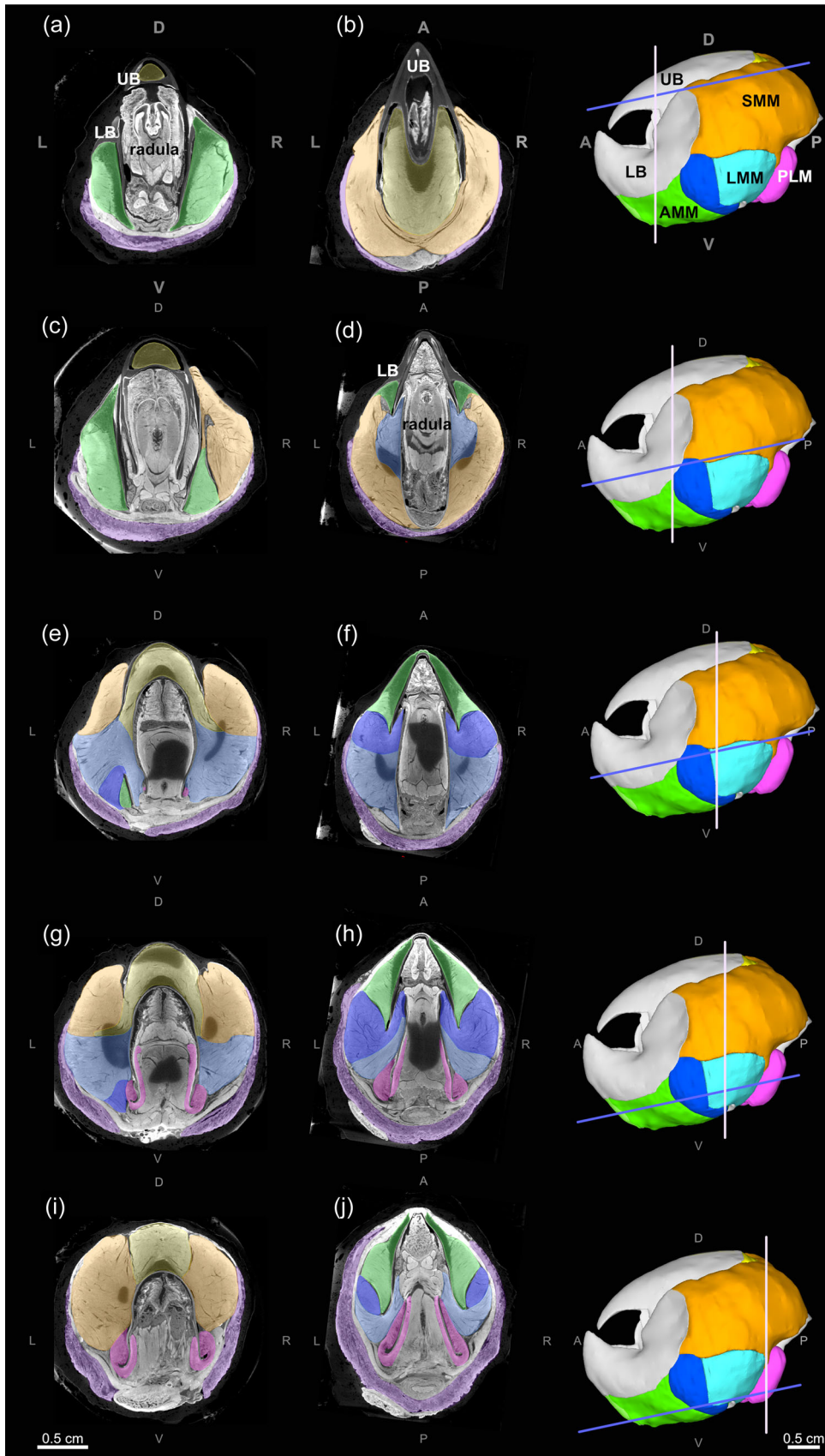
FIGURE 3 (See caption on next page)

consists of the SMM, a pair of AMMs, a pair of LMM, and the PMM. These muscles surrounding the beaks are covered by a buccal sheath, a membrane consisting of connective tissue and epithelium (Tanabe et Fukuda 1999; Supporting Information online Material, Supporting Information: Figure S2). In the following descriptions, figure citations indicate sections in which the focal muscle is the most clearly visible.

The (SMM, in orange and yellow) is the largest mandibular muscle, relative to the weight of the entire buccal mass (Table 1). It can be divided into three divisions (Supporting Information online Material, Supporting Information: Figure S1D). Two divisions (orange) surround the lateral wall of the upper beak on both sides and pass underneath the wings of the lower beak. They are joined to the AMM by a connective tissue sheet. The fibers originate at the very rear of the upper beak crest and descend on either side of the upper beak (SMM, lateral division ex: Figure 2b,c,i). The third division (yellow) is centrally positioned (SMM, central division, ex: Figure 2b, Figure 3e,g, and Figure 4b), originates at the separation between the two previous bundles and inserts onto the upper beak hood on a non-fibrous connective tissue sheet that conforms to the shape of the hood and rostrum (Figure 5b,c). The fibers in the SMM central division run along the antero-posterior axis (Supporting Information online Material, Supporting Information: Figure S1F, 2B3).

The pair of (AMM, in green) appears as a lower extension of the SMM (Figure 2a,c). They are relatively small compared to the entire muscle mass (Table 1). On each side, they are attached to the lateral wall of the lower beak (Figure 3a,c; Supporting Information Online Material, Supporting Information: Figure S1G). A part is hidden under the lower beak wing where it joins the SMM. It appears triangular in lateral view and has three attachment points at its corners. The first two are connected to the SMM and the LMM, while the third involves a connective tissue sheet that binds both AMMs together and inserts inside the lower beak hood (Figure 4d). Fibers follow two directions: a dorso-ventral and an antero-posterior one, and join the three corners of the muscle (Supporting Information Online Material, Supporting Information: Figure S2B, B1).

The pair of (LMM, in blue) is connected to the SMM at the lateral division (Supporting Information Online Material, Supporting Information: Figure S1E). They attach to the lateral walls of the upper and lower beaks and are connected to all the other surrounding muscles (Figure 4E; Supporting Information Online Material, Supporting Information: Figures S1E–H, Figure 2) and the surrounding buccal sheath (Uyeno & Kier, 2005; Supporting Information: Figure 2). Each muscle mass is divided in two divisions. A first bigger one is directly connected to the SMM (LMM main division, in light blue, Figure 4e). The fibers are curved and oriented laterally from the lateral wall of the upper beak to the external side. They are clearly distinct from the other part of the LMM which is smaller (LMM, anterior section, deep blue). This part has longer, straighter fibers which run diagonally toward the posterior part of the beak.

The (PMM, in purple) is superficial compared to others. It surrounds the oesophagus and is connected to the edge of the upper and lower beak hoods, wrapping the entire muscle mass (Supporting Information Online Material, Supporting Information: Figure S1A–C). The fibers are oriented dorso-ventrally between the upper and lower beak crest edges. However, it is difficult to determine which parts contains muscle fibers and which parts are solely connective tissues, at least on the scans and gross dissections. Depending on the species, the fibers follow the entire length of the buccal mass (e.g., *Dosidicus gigas*, Figure 3) or are concentrated between the crest of both beaks (i.e., *I. coindetii*) and completed with connective tissue. Some fibers of this muscle merge with the SMM at its surface, while some are attached to the crest and the hood of the lower beak.

Another pair of muscles is connected to the Superior, Anterior, and LMMs: the Postero-Lateral Muscles (PLM, in pink). These are radular muscles attached to the edge of the lateral walls of the upper beak and connected with the radular apparatus (Supporting Information Online Material, Supporting Information: Figure S2B1). The muscle runs around the edge of the beak and has a long insertion on its lateral wall (Figure 2f and Figure 3h). The muscle is connected to the SMM, AMM and LMM. In *I. coindetii*, the PLM is smaller and rounder (Figure 2h) compared to *Dosidicus gigas* where it is more elongated (Figure 3j).

In *S. officinalis* and *I. coindetii*, the SMM is the muscle with the largest PCSA and can thus produce the greatest forces, the second largest being the LMM (Table 1). In both species, the AMM shows median value of PCSA, while the PMM and PLM show low values. In *Dosidicus gigas*, the relative importance of the PCSA is different, with the LMM being the muscle with the largest PCSA, the second largest being the AMM, and the SMM comes in third position. The PLM in *D. gigas* shows low values compared to the other muscles.

Whereas the general arrangement of the mandibular muscles is similar for all decapodiforms examined, several differences appear to distinguish them from octopodiforms. These differences are emphasized in the description of the octopodiform musculature below.

3.2 | The buccal mass of octopodiforms: O. vulgaris and Eledone cirrhosa

The buccal mass of octopodiforms is made up of five mandibular muscles (SMM, AMM, LMM, PMM, PLMM. *O. vulgaris* (Figure 6) and *Eledone cirrhosa* (Figure 7) represent this muscular organization well.

FIGURE 3 Volume renderings and virtual sections illustrated in different orientations of *Dosidicus gigas* from microCT scan with PMA staining. On the right, the 3D model illustrates the section planes with frontal sections (a–i, white lines) and sagittal section (b–j, blue lines). The muscles are identified by colors. Superior Mandibular Muscle (SMM), lateral division, orange; SMM, inner division, yellow; Anterior Mandibular Muscle (AMM), green; Lateral Mandibular Muscle (LMM), main part, light blue; LMM, anterior section, deep blue; Postero-Lateral Muscle (PLM), pink; Posterior Mandibular Muscle (PMM), purple. The PMM is visible on the sections, yet not illustrated on the 3D model as it surrounds the entire muscle mass and would have masked the other structures. 3D, three dimensional; LB, Lower beak; UB, Upper beak.
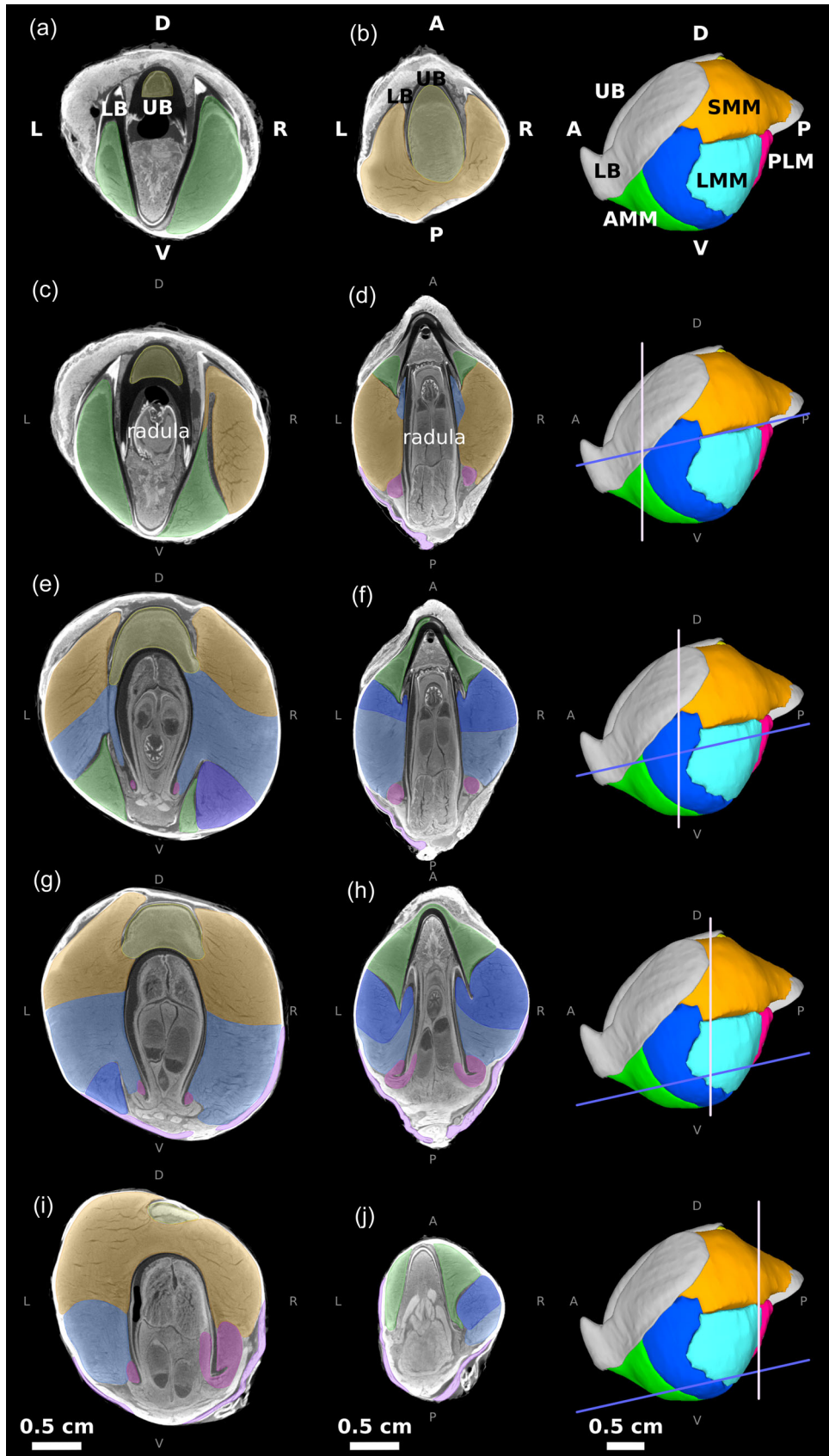
FIGURE 4 (See caption on next page)

The SMM, in orange, is homologous to the SMM in decapodiforms. However, in octopodiforms this muscle is divided into the two lateral sections only. The central section is reduced to a connective tissue sheet attaching the two lateral sections to the hood of the upper beak (Figure 6a,i,j). The fiber orientation of the two main divisions is straight along the antero-posterior axis following the shape of the beak (Figure 6b), similar to the SMM of decapodiforms.

The AMM, in green, is an extension of the SMM. Nevertheless, it is bigger and differently oriented in comparison to the AMM of decapodiforms. The fibers in the AMM and in the SMM are oriented differently (Figure 7d,e) which helps to visualize the separation between the two muscles. Their connection is larger and more robust compared to that observed in decapodiforms. The AMM still appears triangular in lateral view but is bigger, longer and more rounded in octopodiforms. The attachments on the lower beak are the same as in decapodiforms and the muscle bundles follow the lateral walls. The fiber orientations are multiple. They are mainly directed antero-posteriorly, but also perpendicularly to the long axis.

The LMM, in blue, is connected to the SMM. It has a volume comparable to that of the AMM (Table 1). As in decapodiforms, it is attached to the lateral walls of the upper beak and is connected to the SMM, AMM, and the Postero-LMM (PLMM, see below). It is an extension of the SMM and the separation is not clear because the fibers interdigitate. In octopodiforms, this muscle consists of a single bundle. The fibers are oriented diagonally from the lateral wall of the upper beak to the external side and connected to the connective tissue of the SMM at its central part following the hood of the upper beak. In *Eledone cirrhosa* the LMM and the SMM appear more continuous with similar fiber orientations and are less clearly separated.

The PMM, in purple, is a thin muscle situated at the back of the buccal mass. It is homologous and rather similar in form, position and fiber orientation to the PMM of decapodiforms, but even thinner. It surrounds the oesophagus and is attached to the edge of the lower and upper beak hoods (Figure 5a). The muscle fibers are not distributed along the entire length of the buccal mass, however. They are present mostly at the posterior part connecting the two beaks dorso-ventrally. The remainder is mainly made up of connective tissue.

The Postero-LMM (PLMM, in red) is a mandibular muscle attached on the edge of the lateral walls of the upper beak (Figure 6f,h–j). It is not homologous to the PLM in decapodiforms because it is not connected to the radular apparatus and muscle fiber orientations are different (Figure 7a–c). This muscle is therefore unique to octopodiforms and is absent in decapodiforms. It is rounded and connected to the LMM and SMM only. The fibers have three different orientations: antero-posterior, dorso-ventral, and medio-lateral, as visible on the

scans (see scans available on Morphosource.org, ID: 000501081; 000501075; 000501050; 000495791).

In *O. vulgaris*, similar to the observation made in *S. officinalis* and *I. coindetii*, the SMM is the muscle with the largest PCSA (Table 1). However, here, the PLMM is the muscle with the second largest PCSA, showing values similar to the SMM. AMM. The LMM both comes third with a similar PCSA, and the PMM shows again low values compared to the other muscles.

4 | DISCUSSION

The buccal mass of coleoids is composed of four main homologous muscles, the SMM, LMM, AMM, and the PMM. They are present in both decapodiforms and octopodiforms. The SMM is the largest muscle, as described by Kear (1994) and Uyeno and Kier (2007). It has three divisions in decapodiforms, but only two in octopodiforms. Indeed, the central division is not muscular in the latter group but mainly composed of connective tissue attached to the rear of the hood (Figure 5a–c). The central section of this muscle has been suggested to be activated jointly with the LMM during beak opening Kear (1989). The lateral sections of the SMM have been defined as the main closing muscles. As the PCSA is directly correlated with muscle force, we expect the muscle with the largest PCSA to be the ones involved in the closing motion. This is what we observe for the SMM which shows the highest PCSA in most species. Kear (1994) highlighted the importance of beak shape in understanding the anatomy, volume and muscle layout of the buccal masses in different coleoid species. In octopodiforms, the thin central division can be related to the short, narrow, and rounded octopodiform hood. This is in contrast to the more robust central division that is allowed by the wide, elongate hood/rostrum in decapodiforms. For this reason, the SMM in octopodiforms has a smaller relative volume than in decapodiforms.

The PMM is a thin muscle that is attached to the hood and along the posterior edges of the crests and lateral walls. This muscle is likely involved in the beak opening because of its position posterior to the muscle articulation. In decapodiforms, the large size of *Dosidicus gigas* allows to better visualize the complexity of this muscle, being subdivided in several bundles composed of muscle fibers and connective tissue. Depending on the size of the individual and of its buccal mass, these different divisions may not be visible during dissection. The detailed anatomy of this surrounding muscle must be further investigated to understand its function.

FIGURE 4 Volume renderings and virtual sections illustrated in different orientations of *Sepia officinalis* from microCT scan with PMA staining. On the right, the 3D model illustrates the section planes with frontal sections (a–i, white lines) and transversal section (b–j, blue lines). The muscles are identified by colors. Superior Mandibular Muscle (SMM), lateral division, orange; SMM, inner division, yellow; Anterior Mandibular Muscle (AMM), green; Lateral Mandibular Muscle (LMM), main part, light blue; LMM, anterior section, deep blue; Postero-Lateral Muscle (PLM), pink; Posterior Mandibular Muscle (PMM), purple. The PMM is visible on the sections, yet not illustrated on the 3D model as it surrounds the entire muscle mass and would have masked the other structures. 3D, three dimensional; LB, Lower beak; UB, Upper beak.

TABLE 1 Mean muscle mass, proportion of the total mass, and fiber length and PCSA (Physiological Cross Sectional Area) for each dissected species.

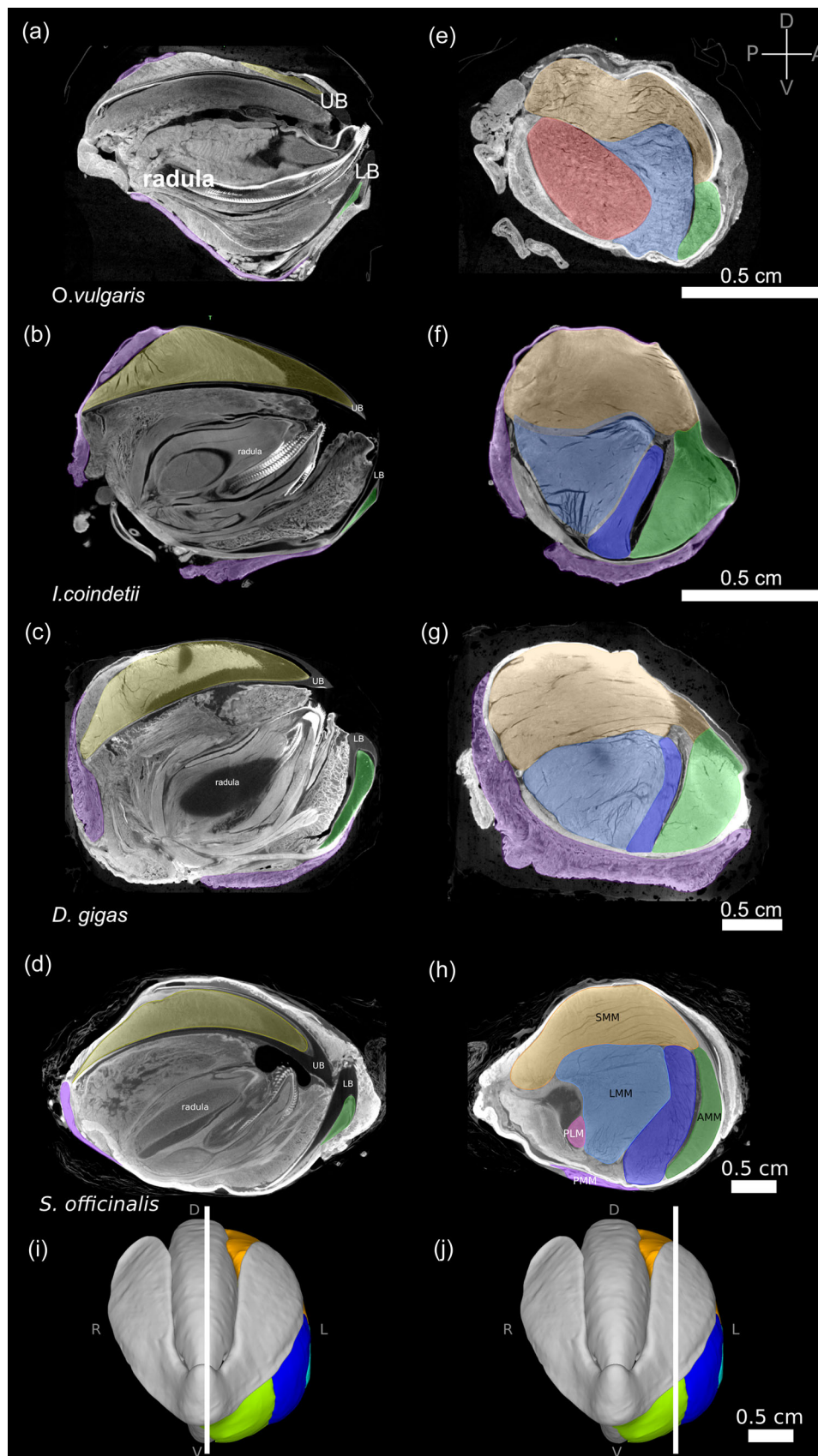| Species	Sepia officinalis					Illex coindetii					Dosidicus gigas					Octopus vulgaris				
N	1					3					1					1				
Muscle	SMM	AMM	PLM	LMM	PMM	SMM	AMM	PLM	LMM	PMM	SMM	AMM	PLM	LMM	PMM	SMM	AMM	PLMM	LMM	PMM
Mean muscle mass (gr)	1.871	0.460	0.186	1.389	0.401	1.260	0.102	0.046	0.440	0.299	30.953	4.944	0.795	17.940	18.505	0.392	0.242	0.380	0.186	0.127
Mass proportions	43.4%	10.6%	4.4%	32.581%	9.4%	58.7%	4.7%	2.2%	20.5%	13.9%	42.3%	6.7%	1.2%	24.5%	25.3%	29.5%	18.2%	28.6%	14.1%	9.6%
Mean fiber length (cm)	1.105	0.556	0.655	0.976	0.966	0.968 ± 0.087	0.333 ± 0.033	0.434	0.751 ± 0.021	2.289	4.226	0.647	0.659	1.831	NA	0.386	0.397	0.410	0.303	0.430
PCSA	1.597	0.780	0.267	1.342	0.391	1.227	0.289	0.099	0.552	0.123	6.909	7.208	1.138	9.243	NA	0.958	0.575	0.859	0.577	0.277

Note: N is the number of dissected specimens.

Abbreviations: AMM, Anterior Mandibular Muscle; LMM, Lateral Mandibular Muscle; PLM, Postero-Lateral Muscle; PLMM, Postero-Lateral Mandibular Muscle; PMM, Posterior Mandibular Muscle; SMM, Superior Mandibular Muscle.

The only insertion of the LMM visible during dissection is on the upper beak lateral wall, but a large insertion onto the surrounding buccal mass sheath was also described Uyeno and Kier (2005) and Uyeno and Kier (2007). Whereas two parts can clearly be identified in decapodiforms based on muscle fiber orientation, only one is clear in octopodiforms (Figure 5d–f). The fiber orientation is also different between the two groups, leading to different functional postulates for this muscle. Given the multiple fiber orientations, this muscle may be involved in beak opening but also in other movements, such as a lateral shear as identified by Uyeno and Kier (2007) and external flexion of the lateral walls of the upper beak (Kear, 1994). This is emphasized by the high PCSA values of this muscle. Beak opening likely does not require great muscles forces suggesting that this function by itself is unlikely to explain the large PCSA observed in all species. The high values observed here suggest an important role of the LMM during the bite, potentially for lateral shearing during the closing motion.

The PLMM is described here as an independent muscle that exists only in octopodiforms. Indeed, this muscle is only attached to the lateral walls of the upper beak. This muscle resembles the LMM described in *Octopus* by Boyle et al. (1979) and Uyeno and Kier (2007) but it cannot be homologous to the LMM of decapodiforms as described by Kear (1994). Even if the PLMM and LMM of octopodiforms are located in an anatomical position that could resemble the one of the two parts of the LMM in decapodiforms (Figure 1e–h and 6e-h) their fiber orientation is different and a clear connective tissue separates the PLMM in octopodiforms from the other muscles. Moreover, the position of this muscle is more similar to that of the PLM in decapodiforms, which is likely a radular muscle given its attachment to the radular apparatus. This PLM has not been described in previous studies of the radula, except for a potential mention in Williams (1909). The interaction between the odontophore complex and the beaks is known to be important, yet, still not validated by in vivo observations (Altman & Nixon, 1970; Young, 1991). The large PCSA values of the PLMM suggest an essential albeit not fully understood role of this muscle in the bite cycle of octopodiforms. This muscle is likely involved in the closing motion of the beaks, yet this remains to be tested.

Studying the fiber orientation and origins and insertions of the different muscles has permitted a better identification of their roles in the bite cycle in different cephalopod species. The lateral divisions of the SMM and the AMM are linked and both span the upper and the lower beaks, thus allowing the beak closure. However, this connection is different for decapodiforms and octopodiforms. Indeed, in octopodiforms, the interweaving between the SMM and the AMM muscle fibers is greater than in decapodiforms where the interface between the two muscles is more reliant on strong connective tissue. Whereas Boyle et al. (1979) described the SMM as the principal closing muscle, Kear (1994) emphasized the potential movement of each different muscle when stimulated independently. The role of these two muscles in beak closure is supported by the studies of Kear (1989) and Uyeno and Kier (2007) using electromyography to demonstrate muscle activity during closure. Kear (1989) suggested

FIGURE 5 Virtual Sagittal sections of *Octopus vulgaris* (a, e); *Illex coindetii* (b, f); *Dosidicus gigas* (c, g) and *Sepia officinalis* (d, h). The muscles are identified by colors. Superior Mandibular Muscle (SMM), lateral division, orange; Anterior Mandibular Muscle (AMM), green; Lateral Mandibular Muscle (LMM), main part, light blue; LMM, anterior section, deep blue; Postero-LMM (PLMM), red; Postero-Lateral Muscle (PLM), pink. (i–j) 3D models in frontal view with white lines illustrating the sagittal planes illustrated above. 3D, three dimensional; LB, Lower beak; UB, Upper beak.
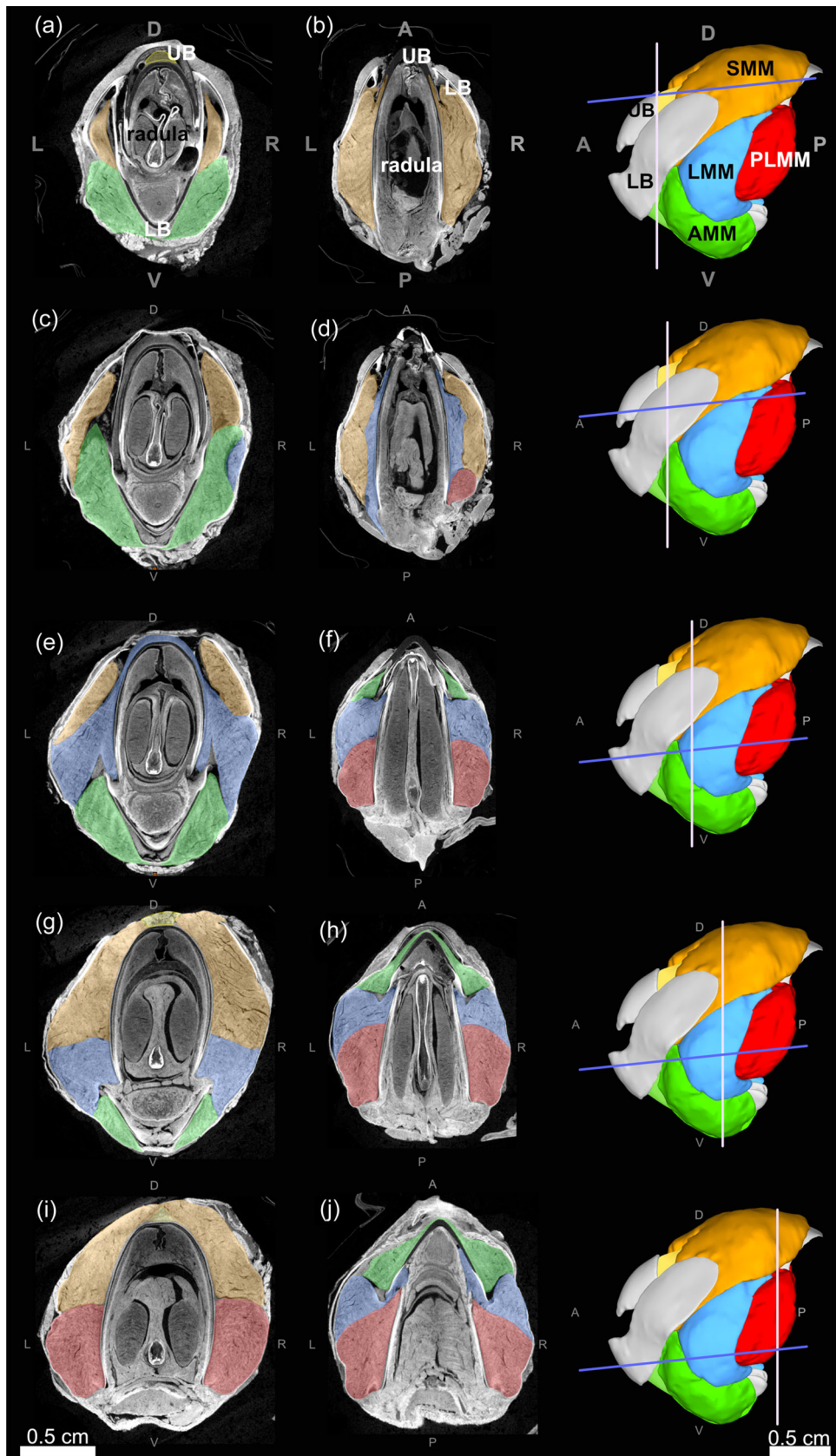
FIGURE 6 Volume renderings and virtual sections illustrated in different orientations of *Octopus* from microCT scan with PMA staining. On the right, the 3D model illustrates the section planes with frontal sections (a–i, white lines) and transversal section (b–j, blue lines). The muscles are identified by colors. Superior Mandibular Muscle (SMM), lateral division, orange; Anterior Mandibular Muscle (AMM), green; Lateral Mandibular Muscle (LMM), light blue; Postero-LMM (PLMM), red; Posterior Mandibular Muscle (PMM), purple. The PMM is visible on the sections, yet not illustrated on the 3D model as it surrounds the entire muscle mass and would have masked the other structures. 3D, three dimensional; LB, Lower beak; UB, Upper beak.
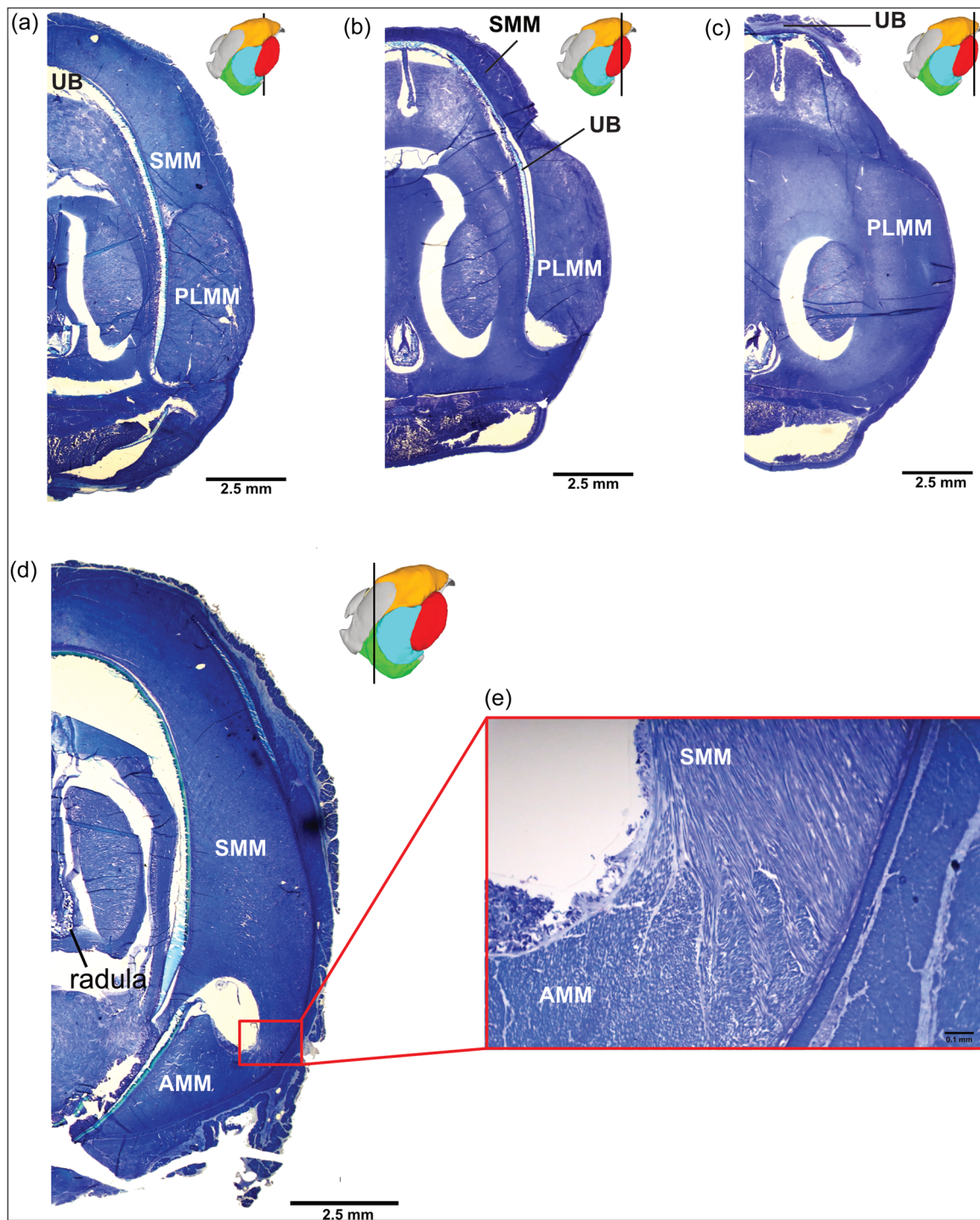
FIGURE 7 Histological sections of *Eledone cirrhosa* showing: (a–c) the position and connections of the PosteroLateral Mandibular Muscle (PMM) specific to octopodiforms, (d, e) the contact zone between the Anterior Mandibular Muscle (AMM) and the Superior Mandibular Muscle (SMM), with (e) a zoom showing the complex connection between the two muscles. The black line on the 3D models shows the position of the frontal section illustrated. 3D, three dimensional; LB, Lower beak; UB, Upper beak.

that the upper beak, with the action of the SMM, is responsible for the translational closure movement whereas the AMM, attached to the lower beak, helps to pull the beaks together and rotates them, creating the shearing motion. Our results are congruent with this

hypothesis and it seems that the lower beak is more mobile than previously assumed (Altman & Nixon, 1970).

Young's (1991) study demonstrated that the radular musculature of *Octopus* is anatomically distinct from that of decapodiforms.

Consequently, the motion and precise function of the radular ribbon might differ between the two groups. Young (1991) further suggested that the manipulation of food by the radula is much more varied and important for food intake in octopodiforms. Combined with our hypotheses of mandibular muscle function, these observations lead us to suggest that there are, at least, two functionally different morphological organizations in coleoid buccal masses. Indeed, comparisons of buccal masses histological sections of various species of octopodiforms and decapodiforms (Nixon & Young, 2003) confirm this observation of a different muscular architecture between the two groups; the arrangement within octopodiforms is preserved across species and similarly so within decapodiforms. Nevertheless, this observation goes against the interpretations of Kear (1994) and Uyeno and Kier (2005) who described differences in muscle volume and shape between mandibular muscles depending on the species but no major functional differences in the muscle architecture and bite cycle.

To further understand the beak and radula function in coleoids new experiments focusing on the major differences between the LMM, PLMM and PLM are needed. In vivo observations of feeding using X-ray videography recordings would be especially insightful and the activation patterns of the different parts of each muscle need to be understood. The potential crushing and piercing functions (Kear, 1989; Roscian et al., 2022) could be investigated with this technique, just as the shearing-like movements described by Uyeno and Kier (2007). The direct observation of the beak and radular motion is needed to understand how these two parts are working together during the bite cycle.

This study is based on muscle data only, but to go further, it could be interesting to include the other parts of the buccal mass, such as the buccal sheath (Uyeno & Kier, 2005), the lips (Kear, 1994) and the brachial crown. Biomechanical models such as multibody dynamics models may provide deeper insights into the function of the different muscle groups. In addition, measures of bite force may complement these analyses when correlated to muscle cross sectional data and may provide insight into the performance of the feeding system in cephalopods. Based on our data showing a considerably different organization of the buccal mass muscles with five mandibular muscles and a strong PLMM in octopodiforms compared to the four mandibular muscles without PLMM in decapodiforms, we predict differences in bite force between these groups. Deciphering the link between beak shape and function is a key to better understand variation in diet and trophic relationships, in adults and in the various developmental stages, ultimately allowing a better understanding of their trophic changes during growth. Finally, these findings will open new horizons for better inferences on past trophic relationships by comparing the shape of actual and extinct species and extrapolating their habitat, trophic level, bite forces and function.

5 | CONCLUSIONS

Our analyses of the buccal masses in representatives of the major groups of coleoid cephalopods show similarities as well as unique features. Octopodiforms have five mandibular muscles with a big

round and strong PLMM, the function of which is not clear. Decapodiforms differ in the organization of the buccal mass by having only four mandibular muscles. Those muscles have also different divisions. In octopodiforms, the SMM is divided in two lateral parts whereas there is a third central section in decapodiforms. This is probably related to hood shape differences between the groups, also suggesting differences in function. Our quantitative data pave the way for future modeling studies, including bite force estimations and distribution of constraints on the beak during the bite cycle, that may provide important insights into the form-function relationships of the buccal mass in coleoid cephalopods.

CONFLICT OF INTEREST STATEMENT

The authors declare no conflict of interest.

DATA AVAILABILITY STATEMENT

The data that support the findings of this study are openly available in MorphoSource at http://n2t.net/ark:/87602/m4/.

CT Scan data are available through MorphoSource (http://n2t.net/ark:/87602/m4/495791; http://n2t.net/ark:/87602/m4/501081, http://n2t.net/ark:/87602/m4/501050, http://n2t.net/ark:/87602/m4/501075) with the technical information of the scan parameters.

ORCID

Marjorie Roscian [ID] http://orcid.org/0000-0002-4290-082X
Louise Souquet [ID] http://orcid.org/0000-0002-0348-4704
Theodore Uyeno [ID] http://orcid.org/0000-0001-8998-5595
Isabelle Rouget [ID] https://orcid.org/0000-0002-9673-0416

PEER REVIEW

REFERENCES

Altman, J. S. & Nixon, M. (1970). Use of the beaks and raduala byoctopus vulgarisin feeding. *Journal of Zoology*, 161(1), 25–38. https://doi.org/10.1111/j.1469-7998.1970.tb02167.x

Boyle, P. R., Mangold, K., & Froesch, D. (1979). The mandibular movements of *Octopus vulgaris*. *Journal of Zoology*, 188(1), 53–67. https://doi.org/10.1111/j.1469-7998.1979.tb03392.x

Clark, A. J. & Uyeno, T. A. (2019). Feeding in Jawless Fishes. In V. Bels, & I. Q. Whishaw (Eds.), *Feeding in Vertebrates. Fascinating Life Sciences* (pp. 189–230). Springer. https://doi.org/10.1007/978-3-030-13739-7_7

Clarke, M. R. (1986). *A Handbook for the Identification of Cephalopod Beaks* (p. 273). Clarendon Press; Oxford University Press.

Cooke, I. R., Whitelaw, B., Norman, M., Caruana, N., & Strugnell, J. M. (2009). Toxicity in cephalopods. In P. Gopalakrishnakone, & A. Malhotra (Eds.), *Evolution of Venomous Animals and Their Toxins* (pp. 125–143. https://doi.org/10.1007/978-94-007-6458-3_7

Davit-Béal, T., Tucker, A. S., & Sire, J. Y. (2009). Loss of teeth and enamel in tetrapods: fossil record, genetic data and morphological adaptations. *Journal of Anatomy*, 214(4), 477–501. https://doi.org/10.1111/j.1469-7580.2009.01060.x

Denton, E. & Gilpin-Brown, J. (1973). Floatation mechanisms in modern and fossil cephalopods. In F. S. Russell & M. Yonge, (Eds), *Advances in Marine Biology* (11, pp. 197–268). Academic Press. https://doi.org/10.1016/S0065-2881(08)60270-9

Descamps, E., Sochacka, A., De Kegel, B., Van Loo, D., Van Hoorebeke, L., & Adriaens, D. (2020). Soft tissue discrimination with contrast agents using micro-CT scanning. *Belgian Journal of Zoology*, 144(1), 20–40. https://doi.org/10.26496/bjz.2014.63

Haxton, H. A. (1944). Absolute muscle force in the ankle flexors of man. *The Journal of Physiology*, 103(3), 267–273. https://doi.org/10.1113/jphysiol.1944.sp004075

Kear, A. J. (1989). Feeding mechanisms and diet in cephalopods: special reference to Antarctic mesopelagic squid, *PhD thesis* (p. 290). University of Aberdeen.

Kear, A. J. (1994). Morphology and function of the mandibular muscles in some coleoid cephalopods. *Journal of the Marine Biological Association of the United Kingdom*, 74(4), 801–822.

Louchart, A. & Viriot, L. (2011). From snout to beak: the loss of teeth in birds. *Trends in Ecology & Evolution*, 26(12), 663–673. https://doi.org/10.1016/j.tree.2011.09.004

Messenger, J. B., & Young, J. Z. (1999). The radular apparatus of cephalopods. *Philosophical Transactions of the Royal Society of London, Series B: Biological Sciences*, 354(1380), 161–182.

Nixon, M. (1979). Has *Octopus vulgaris* a second radula? *Journal of Zoology*, 187(3), 291–296. https://doi.org/10.1111/j.1469-7998.1979.tb03370.x

Nixon, M. (1980). The salivary papilla of octopus as an accessory radula for drilling shells. *Journal of Zoology*, 190(1), 53–57. https://doi.org/10.1111/j.1469-7998.1980.tb01422.x

Nixon, M. (1985). Capture of prey, diet and feeding of *Sepia officinalis* and *Octopus vulgaris* (Mollusca Cephalopoda) from hatchling to adult. *Vie et Milieu*, 35(3), 255–261.

Nixon, M. (2015). Treatise online no. 69: part M, chapter 12: the buccal apparatus of recent and fossil forms. *Treatise Online*. https://doi.org/10.17161/to.v0i0.5047

Nixon, M. & Young, J. Z. (2003). *The brains and lives of cephalopods* (pp. 408). Oxford University Press.

Roscian, M., Herrel, A., Zaharias, P., Cornette, R., Fernandez, V., Kruta, I., Cherel, Y., & Rouget, I. (2022). Every hooked beak is maintained by a prey: Ecological signal in cephalopod beak shape. *Functional Ecology*, 36(8), 2015–2028. https://doi.org/10.1111/1365-2435.14098

Scheel, C., Gorb, S. N., Glaubrecht, M., & Krings, W. (2020). Not just scratching the surface: distinct radular motion patterns in Mollusca. *Biology Open*, 9(10), bio055699. https://doi.org/10.1242/bio.055699

Tanabe, K. & Fukuda, Y. (1999). Morphology and function of cephalopod buccal mass. In E. Savazzi (Ed.), *Functional Morphology of Invertebrate Skeletons* (pp. 245–262). John Wiley Sons.

Tanabe, K. & Fukuda, Y. (2010). Mouth Part Histology and Morphology. In W. B. Saunders, & N. Landman (Eds.), *Nautilus: The Biology and Paleobiology of a Living Fossil* (Vol. 6, pp. 313–322). Springer. https://doi.org/10.1007/978-90-481-3299-7_22

Uyeno, T. A. & Clark, A. J. (2015). Muscle articulations: Flexible jaw joints made of soft tissues. *Integrative and comparative biology*, 55(2), 193–204. https://doi.org/10.1093/icb/icv023

Uyeno, T. A. & Kier, W. M. (2005). Functional morphology of the cephalopod buccal mass: a novel joint type. *Journal of Morphology*, 264(2), 211–222. https://doi.org/10.1002/jmor.10330

Uyeno, T. A. & Kier, W. M. (2007). Electromyography of the buccal musculature of octopus (*Octopus bimaculoides*): A test of the function of the muscle articulation in support and movement. *Journal of Experimental Biology*, 210(1), 118–128. https://doi.org/10.1242/jeb.02600

Uyeno, T. A. & Kier, W. M. (2010). Morphology of the muscle articulation joint between the hooks of a flatworm (Kalyptorhynchia, Cheliplana sp.). *The Biological Bulletin*, 218(2), 169–180. https://doi.org/10.1086/BBLv218n2p169

Voight, J. R. (2012). Suctorial feeding in a deep-sea octopus as a means of niche partitioning (Cephalopoda: Octopodidae). *Zoomorphology*, 132(2013), 157–162. https://doi.org/10.1007/s00435-012-0177-9

Williams, L. W. (1909). The anatomy of the common squid: *Loligo pealii*, Lesueur. (p.112) *The American Museum of Natural History*, https://doi.org/10.5962/bhl.title.11430

Young, J. Z. (1991). The muscular-hydrostatic radula supports of octopus, loligo, sepia and nautilus. *Journal of Cephalopod Biology*, 2(2), 65–81. https://www.jstor.org/stable/56840

SUPPORTING INFORMATION

Additional supporting information can be found online in the Supporting Information section at the end of this article.